Macromolecules

ARTICLE

pubs.acs.org/Macromolecules

A Study on the Kinetics of a Disorder-to-Order Transition Induced by Alkyne/Azide Click Reaction

Xinyu Wei,[†] Le Li,[†] Jeffrey P. Kalish,[†] Wei Chen,[‡] and Thomas P. Russell*[,†]

[†]Department of Polymer Science and Engineering, University of Massachusetts, Amherst, Massachusetts 01003, United States

[‡]Center for Nanoscale Materials, Argonne National Laboratory, Argonne, Illinois 60439, United States

Supporting Information

ABSTRACT: The kinetics of binary blends of poly(ethylene oxide)-*block*-poly(*n*-butyl methacrylate-*random*-propargyl methacrylate) (PEO-*b*-P(nBMA-*r*-PgMA)) diblock copolymer and Rhodamine B azide was investigated during a disorder-to-order transition induced by alkyne/azide click reaction. The change in the domain spacing and conversion of reactants as a function of annealing time were investigated by *in situ* small-angle X-ray scattering (SAXS) and infrared spectroscopy (IR), suggesting several kinetic processes with different time scales during thermal annealing. While a higher conversion can be realized by extending the annealing time, the microphase-separated morphology is independent of the annealing conditions, as long as both the reagents and final products have enough mobility.

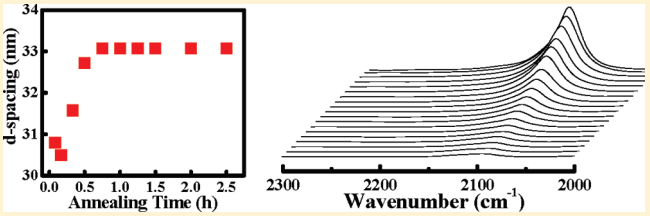

INTRODUCTION

Diblock copolymers (BCPs), consisting of two chemically different chains that are covalently linked at one end, self-assemble into ordered morphologies with feature sizes that are commensurate with the size of the polymer chains and, hence, in the 10−100 nm size scale. The phase behavior of linear, flexible BCPs is dictated by the volume fraction of one block (φ) and the product of χN, where χ is Flory−Huggins segmental parameter, describing the interaction between the two blocks and N is the total degree of polymerization. At low χN, the BCP is in the phase-mixed state, and as χN increases, it undergoes a disorder-to-order transition (DOT); that is, it microphase separates into ordered arrays of lamellar, hexagonally packed cylindrical, or body-centered cubic spherical microdomains or into a bicontinuous gyroid morphology, determined by the volume fraction of each component.[1−4] Therefore, microphase-separated morphologies are emerging as versatile templates and scaffolds for the fabrication of nanostructured materials.[5−10]

One current challenge in developing BCP templates is to generate smaller feature sizes, which enable fabrication of nanostructured materials with higher areal densities. To achieve the highest areal densities, the size scale and pitch of the feature and, hence, the total degree of polymerization must be decreased since, in the strong segregation regime, the pitch of BCP microdomain morphology, D, is governed by the relationship $D \sim N^{2/3}\chi^{1/6}$.[1,3,4] However, as N decreases, the value of χN also decreases and the BCP may disorder; consequently, χ needs to be increased. In fact, the smallest domain size that can be reached is dictated by the magnitude of χ. For instance, polystyrene-*block*-poly(methyl methacrylate) (PS-*b*-PMMA), an ideal material to generate nanoporous templates,[11−14] has relatively weak nonfavorable interaction between the PS and PMMA segments, making it difficult to achieve structures with feature sizes <13 nm.[15,16]

Recently, it has been suggested that χ values of BCPs can be significantly increased by incorporating additives that selectively associate with one block via specific interactions such as metal ion coordination[17−22] and hydrogen bonding.[23−28] Because of the existence of specific interactions, a binary blend of the BCP with additives will behave like a typical BCP, only with a substantially increased value of χ. For example, Wang et al. reported that microphase separation can be induced by the addition of lithium salts to a phase mixed PS-*b*-PMMA BCP.[29] They confirmed that lithium ions could selectively coordinate with the PMMA block, which led to an increase in χ between the two blocks.[30] Tirumala et al. have also reported that a DOT of poly(ethylene oxide)-*b*-poly(propylene oxide)-*b*-poly(ethylene oxide) (PEO-*b*-PPO-*b*-PEO) triblock copolymer was induced by blending with a poly(acrylic acid) (PAA) homopolymer. PAA can selectively hydrogen bond with the PEO block, and the nonfavorable interaction between PPO and complexed PEO is much stronger than the interaction between PEO and PPO. As a result, microphase separation of the triblock copolymer was achieved with its domain size as small as 5 nm.[24,25] Perhaps the smallest domain size yet to be obtained by this route was achieved by Park and co-workers using PS-*b*-PEO, where the PEO was complexed with gold salt and domains as small as 3 nm were obtained.[31]

Previously, we have reported a novel strategy to increase the χ values using alkyne/azide click reaction,[32] i.e., the reaction between

Received: February 8, 2011
Revised: April 21, 2011
Published: May 10, 2011

ACS Publications © 2011 American Chemical Society

dx.doi.org/10.1021/ma200294g | *Macromolecules* 2011, 44, 4269–4275

Scheme 1. Click Reaction between PEO-*b*-P(nBMA-*r*-PgMA) BCP and Rhodamine B Azide

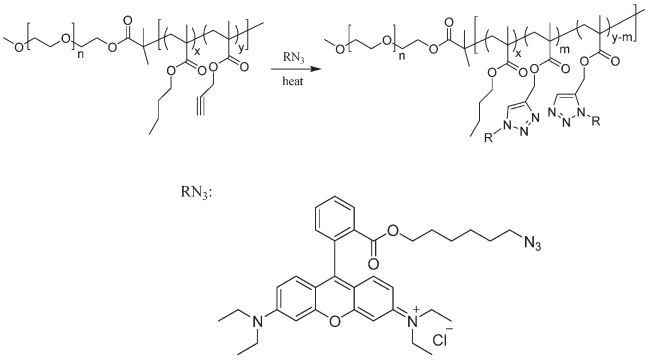

terminal alkynes and azides to form 1,2,3-triazole linkages.[33−35] A poly(ethylene oxide)-*block*-poly(*n*-butyl methacrylate-*random*-propargyl methacrylate) (PEO-*b*-P(nBMA-*r*-PgMA)) BCP was synthesized, and the neat BCP was found to be in a phase-mixed state. It was then blended with an azide compound Rhodamine B azide, annealed at elevated temperatures, and microphase separation was observed.[32] The driving force for such a morphological transition was the significant change in chemical structures due to the click reaction during thermal annealing, which led to an increase of the nonfavorable interaction between the two blocks and thus microphase separation occurred (Scheme 1).[36] In this article, we have investigated the kinetics of the click reaction and the corresponding evolution of the morphology.

EXPERIMENTAL SECTION

Materials. PEO-*b*-P(nBMA-*r*-PgMA) BCP and Rhodamine B azide were synthesized as previously reported.[32] The BCP had a molecular weight of 19 kg/mol for the PEO block, 10 kg/mol for the P(nBMA-*r*-PgMA) block, and a polydispersity index of 1.10. On average, each polymer chain has 33 PgMA repeating units. A P(nBMA-*r*-PgMA) random copolymer was synthesized using a similar polymerization method (see Supporting Information for detailed procedures). All other chemicals were purchased from commercial sources in highest purity and used as received.

Sample Preparation. PEO-*b*-P(nBMA-*r*-PgMA) and Rhodamine B azide were weighed separately according to a certain mole ratio between the alkyne groups in the BCP and the azides, dissolved together in dichloromethane, a good solvent for both components, and then drop-cast onto the substrates. Samples for X-ray scattering characterization, thermal analysis, and electron microscopy observation were prepared by drop-casting a 5 wt % solution onto Kapton films. Samples for IR spectroscopy and optical microscopy experiments were prepared by drop-casting a 1.5 wt % solution onto KBr pellets and glass slides, respectively. All the samples were dried under vacuum to remove residual solvent before subsequent annealing or measurements.

Instrumentation. Gel permeation chromatography (GPC) was measured in tetrahydrofuran (THF) relative to poly(methyl methacrylate) standards (Scientific Polymer Products) on a system equipped with a three-column set (Polymer Laboratories 300 × 7.5 mm; 5 μm; 10^{-5}, 10^{-4}, and 10^{-3} Å pore sizes) and a refractive index detector (HP 1047A) at room temperature with a flow rate of 1 mL/min. Proton nuclear magnetic resonance (^{1}H NMR) spectra were recorded on DPX400 spectrometer in $CDCl_3$.

Differential scanning calorimetry (DSC) experiments were performed using a TA Instruments Q200 instrument under He purge (25 mL/min). About 5 mg of sample was sealed in an aluminum hermetic pan and cycled at 10 °C/min between −100 and 150 °C. Data from the third heating/cooling cycle were used for analysis to minimize the effects of thermal history. Thermal gravimetric analysis (TGA) experiments were performed under a N_2 atmosphere at a heating rate of 10 °C/min.

Fourier transform infrared (FT-IR) spectra were recorded on a Bruker Tensor 27 FT-IR spectrometer by coadding 32 scans in the standard wavenumber range of 400−4000 cm^{-1} at a resolution of 4 cm^{-1}. For *in situ* measurements, the samples were heated under a N_2 atmosphere, and the temperatures were controlled using a home-built hot stage.

Two-dimensional small-angle X-ray scattering (SAXS) experiments were preformed at beamline X27C, National Synchrotron Light Source (NSLS), Brookhaven National Laboratory (BNL). The wavelength of incident X-ray was 0.1371 nm. The sample-to-detector distance was 1816.6 mm. Scattering signals were collected by a marCCD detector, and typical exposure time was 30−90 s. For temperature-dependent experiments, the samples were mounted onto an Instec HCS410 hot stage equipped with liquid-nitrogen cooling and nitrogen gas purging accessories. Two-dimensional wide-angle X-ray scattering (WAXS) experiments were performed at Materials Research Science and Engineering Center (MRSEC) at University of Massachusetts, Amherst, using a WAXS instrument with a three-pinhole collimation system and an Osmic MaxFlux X-ray source (Cu Kα, 0.154 nm). The sample-to-detector distance was 139.0 mm. All WAXS experiments were performed under vacuum at room temperature. Scattering signals were first collected using a Fuji image plate and then transferred into digital images using a Fuji BAS-2500 scanner, with typical exposure time between 60 and 90 min. All SAXS and WAXS data presented here are raw data without background subtraction and empty cell scattering calibration. One-dimensional SAXS and WAXS profiles were obtained by integration of corresponding two-dimensional scattering patterns.

Polarized and fluorescence optical micrographs were imaged using an Olympus model BX60 microscope with a 10× objective in bright field mode and with excitation at ∼450 nm and emission at ∼560 nm, respectively.

To observe the microstructures by transmission electron microscopy (TEM), the blend samples were embedded into an epoxy resin and cured at room temperature for 24 h. Ultrathin sections with thicknesses of 50−70 nm were obtained by cryo-microtomy (Leica Ultracut) using a diamond knife at −60 °C to ensure that no alteration of the morphology took place during cutting. To enhance contrast, the TEM samples were stained by exposure to the vapor of 4 wt % OsO_4 aqueous solution for 1 h. The double bonds in the triazole group formed by click reaction were selectively stained with OsO_4 and appeared dark. Bright field TEM measurements were performed with a JEOL 200CX electron microscope operated at an accelerating voltage of 200 kV.

RESULTS AND DISCUSSION

Morphology Evolution during Click Reaction. Previously, we performed a control experiment using Rhodamine B (no azido functionality) and no microphase separation was observed, indicating that the DOT is due to the click reaction rather than other types of specific interaction.[32] In most previous reports on binary blends of BCPs and specific-interacting additives, the samples were prepared by dissolving the two components in their cosolvents, and specific interactions were formed before subsequent annealing. Here, the alkyne and azide groups do not react with each other until they are heated to elevated temperatures. Therefore, it is crucial to understand the morphological transition

from the disordered state to microphase separation state during thermal annealing. *In situ* SAXS experiments were then performed to provide a real-time observation of the changes in morphology as a function of time and temperature.

DSC traces of the neat PEO-*b*-P(nBMA-*r*-PgMA) BCP exhibited an endothermic peak at 50 °C during heating and an exothermic peak at 15 °C during cooling (Figure S1), suggesting crystal melting and recrystallization. The glass transition of the BCP was not detected. WAXS profile of the neat BCP (Figure 1a) revealed four discrete diffraction peaks with positions at q = 13.6, 16.6, 18.5, and 19.0 nm^{-1}, corresponding to d-spacings of 0.462, 0.379, 0.340, and 0.331 nm, respectively. These peak positions are in good agreement with the 120, 032, 224, and 024 reflections of PEO homopolymer.[37] Polarized optical microscopy images of both the as-cast and thermally annealed samples showed a spherulitic morphology (Figure S2). These results suggest that the PEO block in the BCP crystallized and the crystal structure was not affected by the incorporation of P(nBMA-*r*-PgMA) block. Therefore, the temperature for annealing has to be above the melting point of PEO block. Since the TGA analysis of Rhodamine B azide (Figure S3) shows a weight loss beginning at 150 °C, an annealing temperature was chosen not to exceed 150 °C to prevent thermal degradation of the azide.

We first investigated the morphological evolution at 110 °C, since we observed the DOT induced by the alkyne/azide click reaction previously at this temperature.[32] The BCP was blended with Rhodamine B azide at a mole ratio of 1:1 between the alkyne groups and azide groups, to be consistent with previous conditions. The blend was then heated, and scattering profiles were collected during the annealing process. Figure 2a shows the SAXS profiles at different annealing times. The as-cast sample

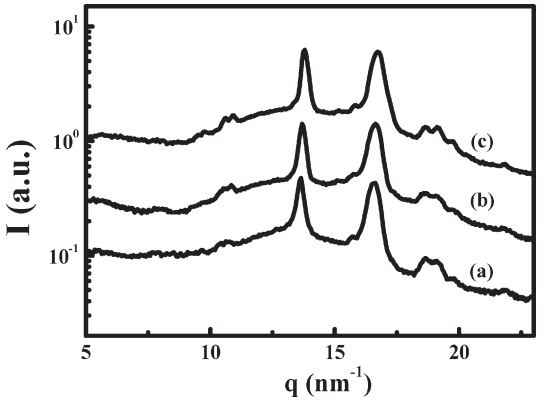

Figure 1. WAXS profiles of (a) neat PEO-*b*-P(nBMA-*r*-PgMA) BCP annealed at 130 °C for 12 h; (b) binary blend of PEO-*b*-P(nBMA-*r*-PgMA) and Rhodamine B at a mole ratio of 1:1 between the alkyne and azide groups, drop-cast from 5 wt % solution in dichloromethane; (c) the same blend sample as in (b) after annealing at 110 °C for 12 h.

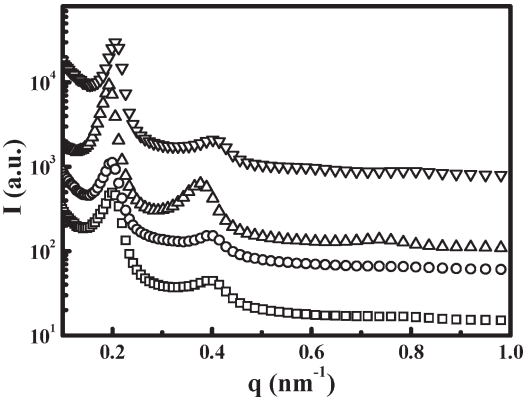

Figure 3. SAXS profiles of binary blends of PEO-*b*-P(nBMA-*r*-PgMA) and Rhodamine B azide anneald at 110 °C for 12 h (□), 24 h (○), and 36 h (Δ) and at 130 °C for 48 h (▽). The mole ratio between the alkyne groups and azide groups was 1:1.

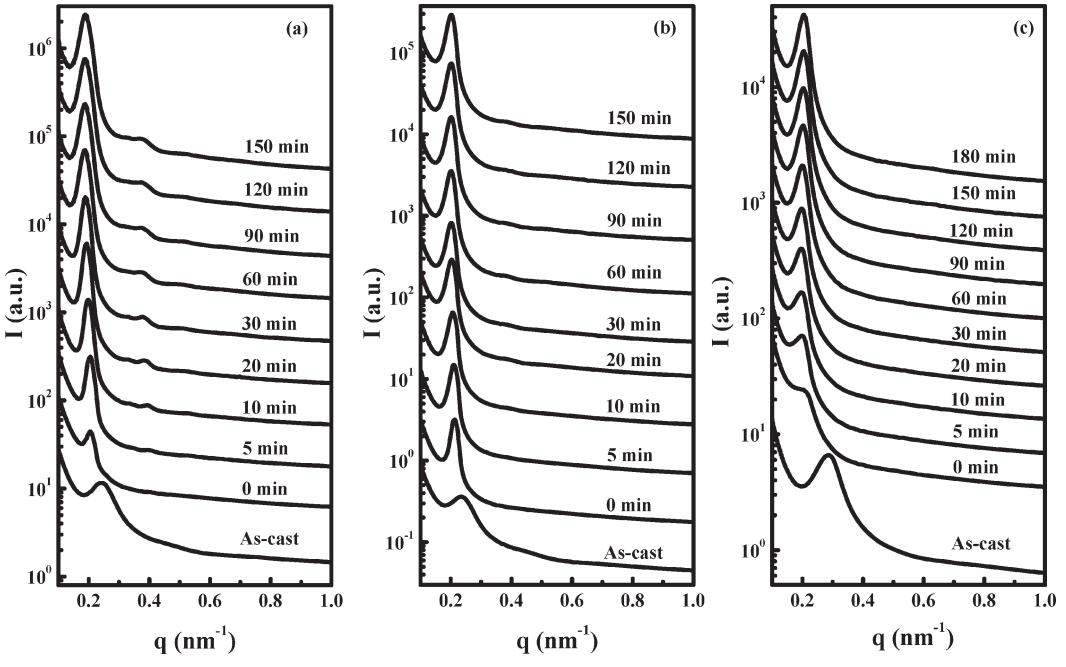

Figure 2. *In situ* SAXS profiles of binary blends of PEO-*b*-P(nBMA-*r*-PgMA) and Rhodamine B azide at 110 (a), 90 (b), and 70 °C (c). The mole ratio between the alkyne groups and azide groups was 1:1.

dx.doi.org/10.1021/ma200294g |*Macromolecules* 2011, 44, 4269–4275

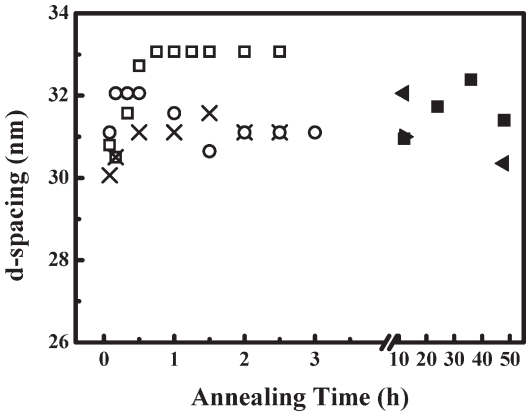

Figure 4. Domain spacing of binary blends of PEO-*b*-P(nBMA-*r*-PgMA) and Rhodamine B azide, after annealing at 110 (□, ■), 130 (left-pointing ▲), 150 (right-pointing ▲), 90 (×), and 70 °C (○). The mole ratio between the alkyne groups and azide groups was 1:1. Open symbols correspond to data from *in situ* measurements, and solid symbols correspond to data measured from individual samples at different annealing conditions.

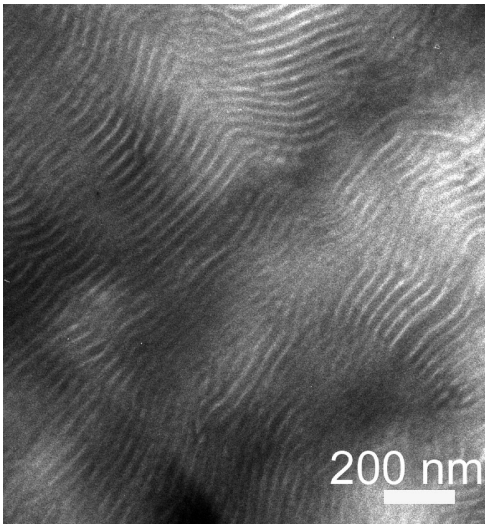

Figure 5. Cross-sectional TEM image of a binary blend of PEO-*b*-P(nBMA-*r*-PgMA) and Rhodamine B azide after annealing at 110 °C for 36 h. The mole ratio between the alkyne groups and azide groups was 1:1.

exhibited a broad peak at $q \sim 0.28$ nm^{-1}, which is due to the crystalline lamellae of the PEO block. After the sample was heated to 110 °C, the initial broad peak disappeared, and a new peak emerged at $q = 0.21$ nm^{-1}. As the annealing time increased, the peak position shifted slightly to 0.19 nm^{-1}, corresponding to a domain spacing of 33 nm, and remained constant. After annealing at 110 °C for ~20 min, another peak was observed at 0.38 nm^{-1}. Since the position of the second peak is twice of the q value of the first-order peak, we conclude that a lamellar morphology is present, in good agreement with our previous observations. Parts b and c of Figure 2 show the *in situ* SAXS profiles of the blend when annealed at 90 and 70 °C, respectively. Similarly, microphase separation was observed shortly after the sample was heated to the targeted temperatures. We also investigated samples annealed at different temperatures for

Figure 6. Polarized optical microscopy images (a, c) and fluorescence optical microscopy image (b) of a binary blend of PEO-*b*-P(nBMA-*r*-PgMA) and Rhodamine B azide before (a, b) and after (c) annealing at 110 °C for 12 h. The mole ratio between the alkyne groups and azide groups was 1:1.

prolonged annealing times. As can be seen in Figures 3 and 4, all the samples showed a lamellar morphology after thermal annealing, with the domain spacing between 31 and 33 nm. Therefore, we can conclude that the DOT induced by alkyne/azide click chemistry has fast kinetics with no obvious intermediate state. The morphology after the click reaction is independent of the annealing temperature and annealing time. Microphase separation induced by the click reaction was also confirmed by cross-section TEM, as shown in Figure 5. The triazole group formed by the click reaction was selectively stained with OsO_4 and appeared dark.

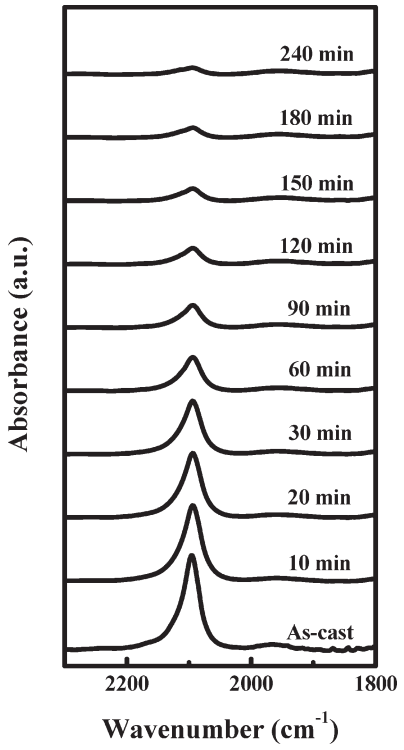

Figure 7. *In situ* FT-IR spectra profiles of a binary blend of PEO-*b*-P(nBMA-*r*-PgMA) and Rhodamine B azide at 110 °C. The mole ratio between the alkyne groups and azide groups was 1:1.

Since the BCP and the azide do not react with each other at room temperature, it is important to investigate the morphology in as-cast blend samples. If the BCP phase separates from the azide, the interface may affect the reactivity and kinetics of the click reaction. Figure 6a shows the polarized optical microscopy image of the as-cast sample showing spherulitic structures. WAXS profiles of the as-cast blend sample (Figure 1b) revealed sharp reflections with peak positions identical to the neat BCP, suggesting that the crystals observed are only from the PEO block and the Rhodamine B azide neither crystallizes by itself nor co-crystallizes with PEO. Since Rhodamine B azide has fluorescence activity, the sample was also examined by fluorescence optical microscopy, and a uniform distribution of fluorescence intensity was observed (Figure 6b), indicating no aggregation of the azide at the micrometer scale. On the basis of these observations, we can conclude that, upon casting, Rhodamine B azide was incorporated into the amorphous region between the PEO crystal lamellae, similar to the morphology reported in blends of PEO and poly(methyl methacrylate) (PMMA).[38,39] After annealing at 110 °C for 12 h, sharp reflections were seen in the WAXS profile (Figure 1c) with peak positions the same as the neat diblock copolymer, suggesting the crystallization of PEO in the modified BCP during cooling without any change in crystal structure. Crystallization of the PEO block after click reaction was also confirmed by DSC (Figure S4), and the glass transition of P(nBMA-*r*-PgMA) block after click reaction was not observed. No spherulites were observed after thermal annealing (Figure 6c), and no change in microphase separation morphology was found when the annealed sample was heated above T_m of PEO block (data not shown). These results suggest that, after the click reaction, crystallization of PEO is confined within nanoscopic domains and cannot form spherulites.[37,40]

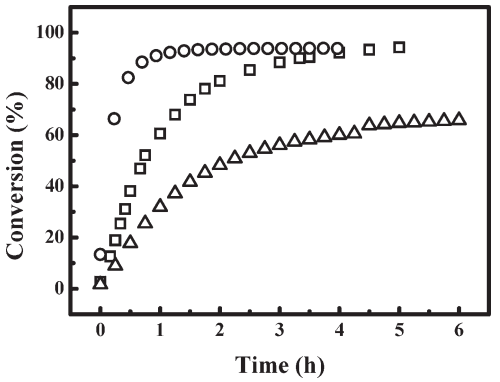

Figure 8. Conversion of the azide groups in the binary blends of PEO-*b*-P(nBMA-*r*-PgMA) and Rhodamine B azide as a function of annealing time at 110 (□), 130 (○), and 90 °C (Δ). The mole ratio between the alkyne groups and azide groups was 1:1.

Kinetics Study of Click Reaction. Although alkyne/azide click chemistry has been widely used, there are few reports on the reaction kinetics and its effects on polymer properties. Recently, Binauld et al. reported a kinetics study of solution-based step growth polymerization of monomers with α,ω-dialkyne or diazido functionality. Conversion of the monomers was monitored by ^{1}H NMR, and first-order kinetics was found with an activation energy of 45 ± 5 kJ/mol.[41] Sheng et al. used thermal analysis methods to investigate similar "click" polymerization catalyzed by Cu(I) salt without solvent.[42] Wu and coworkers studied the mechanism of Cu(I)-catalyzed alkyne/azide click chemistry using real-time IR and suggested that the rate-determining step was the transform of alkyne/azide complex to 1,2,3-triazole.[43]

Previously, we confirmed the click reaction between the alkyne-bearing BCP and Rhodamine B azide by FT-IR spectroscopy, where the stretching vibration peak of azido groups at 2100 cm^{-1} disappeared after thermal annealing.[32] Here we use *in situ* FT-IR spectroscopy to further monitor the reaction process. Figure 7 shows the IR spectra of a binary blend of the BCP and Rhodamine B azide at different annealing times, where the mole ratio between alkyne groups and azide groups was kept at 1:1 and the annealing temperature was 110 °C. It is clear that as the annealing time increased, the absorbance of azido stretching vibration peak decreased significantly, indicating the consumption of azide group due to the click reaction. The conversion of the azido group at different annealing time was calculated according to the integration area of the azido group stretching vibration peak:

$$\text{conversion}\ (\%) = A(t)/A(0) \qquad (1)$$

where $A(t)$ is the integration area of azido stretching vibration peak at a certain annealing time and $A(0)$ is the integration area of the same peak before annealing. As shown in Figure 8, when the blend was annealed at 110 °C, there was initially a sharp increase in conversion up to ~2.5 h with conversion around 91%, followed by a significant decrease in the slope and finally a plateau region, indicating fast kinetics and high conversion. Similar reaction kinetics were reported in a recent study on thermal click reaction of α-azide-ω-alkyne dianhydrohexitol, which showed that the compound could undergo step growth polymerization and monomers could be consumed in a short period of time (3−6 h) at moderate temperatures.[44] Katritzky et al. also

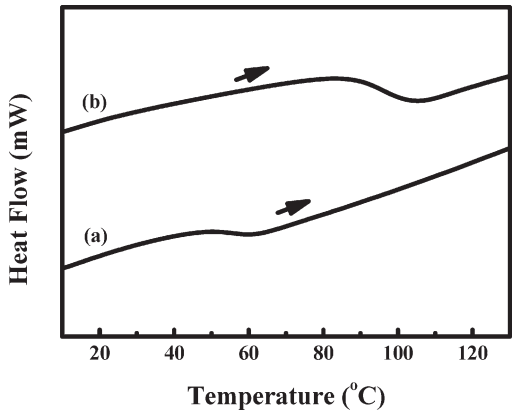

Figure 9. DSC traces of (a) the neat P(nBMA-*r*-PgMA) random copolymer and (b) a binary blend of the copolymer and Rhodamine B azide at 1:1 mole ratio between the alkyne and azide groups, after annealing at 110 °C for 12 h.

studied the click reaction of alkyne and azide end-capped polyols in the absence of solvent and Cu(I) catalyst and reported good kinetics and conversion for most reactions between room temperature and 80 °C.[45] Our results also suggested that without solvent and catalyst the alkyne/azide click reaction can still exhibit a fast reaction rate and high conversion.

We also studied reaction kinetics at 90 and 130 °C. The conversion of the azide groups at different annealing temperature was also calculated using eq 1 and plotted in Figure 8. It can be seen that when the blend was annealed at 130 °C, a more rapid consumption of azides was observed, but the final conversion was similar. When the reaction temperature was decreased to 90 °C, the reaction was much slower, and after 6 h only a 63% conversion was achieved. Recently, a study on the "click" step growth polymerization suggested that once the glass transition temperature of the growing polymer was above the reaction temperature, the system became glassy and further chain growth was significantly suppressed,[44] which is similar to our observations. However, DSC analysis of annealed sample (Figure S4) showed only the characteristic thermal properties of PEO block. Since the melting point of the PEO block after the click reaction was ~60 °C, it should be completely molten at 90 °C and thus would not suppress the reaction. To assess the change in the thermal properties of the P(nBMA-*r*-PgMA) block after the click reaction, a P(nBMA-*r*-PgMA) random copolymer was synthesized. On the basis of ^{1}H NMR and GPC characterizations, the random copolymer has a number-average molecular weight of 18 kg/mol and a polydispersity index of 1.37. On average, each polymer chain has 64 nBMA repeating units and 72 PgMA repeating units, and the ratio between the two comonomers is close to that in the BCP. Figure 9 shows the DSC traces of the neat random copolymer and the copolymer after the reaction with Rhodamine B azide. It is clear that the neat copolymer has a glass transition of ~55 °C. However, after the click reaction, the glass transition temperature increased to ~95 °C. This difference may be due to the reduction of chain mobility after the attachment of bulky Rhodamine B groups. Therefore, we can conclude that at the reaction temperature of 90 °C the modified P(nBMA-*r*-PgMA) block vitrifies and impedes the reaction of the remaining BCP and azides, thus limiting the conversion. In addition, since the T_g of P(nBMA-*r*-PgMA) block after click reaction is much higher than the melting point of the PEO block, crystallization of PEO is confined within the glassy P(nBMA-*r*-PgMA) microdomains and will not disrupt the microphase-separated morphology, which is in agreement with previous observations.[37,40,46,47]

On the basis of the *in situ* observations, we can describe the kinetic properties of the DOT induced by click reaction. As the blend is heated to elevated temperatures, some polymer chains can overcome the energy barrier and react with the surrounding azide compounds. The reaction proceeds more in a "statistical" way than in a "step-growth" way; that is, the alkyne groups in one polymer chain can be fully coupled with the azides very rapidly. The modified BCP chain will then undergo microphase separation, which is also a rapid process. This would explain the result that, while it takes a few hours for the azides to be completely consumed, microphase separation can be observed very early during thermal annealing, and the domain spacing does not change as the annealing time increases. To better understand the kinetics of the click reaction, we performed TEM measurements on a blend sample with short annealing time (~2 h at 110 °C) and thus incomplete consumption of the azides. As can be seen from Figure S5, both phase-separated regions and phase-mixed regions can be observed, which further confirms the kinetics properties. In addition, we attempted to blend the BCP with very small amount of azide, and after thermal annealing, microphase separation was not observed (data not shown). A possible reason is that when only a small amount of alkyne groups are coupled with the azide, the overall segmental interactions are still favorable. This further suggests that the click reaction does not proceed in a step-growth manner. The microphase separation is also independent of annealing temperature. However, both the reagents and the final products need to have sufficient mobility to achieve a good conversion. In addition, although the azide is miscible with the BCP in the as-cast samples, macrophase separation must be considered when other azide compounds are used.

CONCLUSION

The kinetics of the DOT of BCPs induced by alkyne/azide click chemistry has been investigated. The alkyne-bearing BCP and Rhodamine azide are miscible in the as-cast state, and the azide is incorporated into the amorphous regions between PEO crystal lamellae. *In situ* time-resolved SAXS and IR spectroscopy suggest that the BCP has high reactivity and the fast reaction rate with the azide compound at elevated temperatures. Microphase separation can appear in the early stage of thermal annealing, and the morphology is independent of the annealing conditions. These results indicate fast kinetics of both the coupling between a single polymer chain and the azides and the subsequent microphase separation of the modified BCP, while it takes much longer time for all the BCPs and azides to react with each other. In addition, the annealing temperature does not affect the morphology after the click reaction, but it has to be above the glass transition temperature and melting point of both reagents and final products to achieve a fast reaction rate and high conversion.

ASSOCIATED CONTENT

Supporting Information. Synthetic procedures for the preparation of the P(nBMA-*r*-PgMA) random copolymer; DSC traces of the neat diblock copolymer and annealed blend samples; polarized optical microscopy images of the neat diblock

copolymer; TGA analysis of Rhodamine B azide. This material is available free of charge via the Internet at http://pubs.acs.org.

AUTHOR INFORMATION

Corresponding Author
*E-mail: russell@mail.pse.umass.edu.

ACKNOWLEDGMENT

This work was supported by the Department of Energy Office of Basic Energy Science under Contracts DE-FG02-96ER45612 and DE-FG02-04ER46126 and the NSF-supported Materials Research Science and Engineering Center at UMass. Use of the National Synchrotron Light Source, Brookhaven National Laboratory, was supported by the U.S. Department of Energy, Office of Science, Office of Basic Energy Sciences, under Contract DEAC02-98CH10886.

REFERENCES

(1) Bates, F. S.; Fredrickson, G. H. *Annu. Rev. Phys. Chem.* **1990**, *41*, 525–557.
(2) Fredrickson, G. H.; Bates, F. S. *Annu. Rev. Mater. Sci.* **1996**, *26*, 501–550.
(3) Bates, F. S.; Fredrickson, G. H. *Phys. Today* **1999**, *52*, 32–38.
(4) Hamley, I. W. *The Physics of Block Copolymers*; Oxford University Press: New York, 1998.
(5) Fasolka, M. J.; Mayes, A. M. *Annu. Rev. Mater. Res.* **2001**, *31*, 323–355.
(6) Hawker, C. J.; Russell, T. P. *MRS Bull.* **2005**, *30*, 952–966.
(7) Bang, J.; Jeong, U.; Ryu, D. Y.; Russell, T. P.; Hawker, C. J. *Adv. Mater.* **2009**, *21*, 4769–4792.
(8) Segalman, R. A. *Mater. Sci. Eng.* **2005**, *R48*, 191–226.
(9) Li, M.; Ober, C. K. *Mater. Today* **2006**, *9*, 30–39.
(10) Park, C.; Yoon, J.; Thomas, E. L. *Polymer* **2003**, *44*, 6725–6760.
(11) Mansky, P.; Liu, Y.; Huang, E.; Russell, T. P.; Hawker, C. J. *Science* **1997**, *275*, 1458–1460.
(12) Huang, E.; Pruzinsky, S.; Russell, T. P.; Mays, J.; Hawker, C. J. *Macromolecules* **1999**, *32*, 5299–5303.
(13) Ryu, D. Y.; Shin, K.; Drockenmuller, E.; Hawker, C. J.; Russell, T. P. *Science* **2005**, *308*, 236–239.
(14) Thurn-Albrecht, T.; Schotter, J.; Kastle, C. A.; Emley, N.; Shibauchi, T.; Krusin-Elbaum, L.; Guarini, K.; Black, C. T.; Tuominen, M. T.; Russell, T. P. *Science* **2000**, *290*, 2126–2129.
(15) Russell, T. P.; Hjelm, R. P.; Seeger, P. A. *Macromolecules* **1990**, *23*, 890–893.
(16) Xu, T.; Kim, H. C.; DeRouchey, J.; Seney, C.; Levesque, C.; Martin, P.; Stafford, C. M.; Russell, T. P. *Polymer* **2001**, *42*, 9091–9095.
(17) Ruzette, A. V. G.; Soo, P. P.; Sadoway, D. R.; Mayes, A. M. *J. Electrochem. Soc.* **2001**, *148*, A537–A543.
(18) Epps, T. H.; Bailey, T. S.; Pham, H. D.; Bates, F. S. *Chem. Mater.* **2002**, *14*, 1706–1714.
(19) Kim, S. H.; Misner, M. J.; Yang, L.; Gang, O.; Ocko, B. M.; Russell, T. P. *Macromolecules* **2006**, *39*, 8473–8479.
(20) Wang, J.-Y.; Xu, T.; Leiston-Belanger, J. M.; Gupta, S.; Russell, T. P. *Phys. Rev. Lett.* **2006**, *96*, 128301/1–128301/4.
(21) Lee, D. H.; Kim, H. Y.; Kim, J. K.; Huh, J.; Ryu, D. Y. *Macromolecules* **2006**, *39*, 2027–2030.
(22) He, J.; Wang, J.-Y.; Xu, J.; Tangirala, R.; Shin, D.; Russell, T. P.; Li, X.; Wang, J. *Adv. Mater.* **2007**, *19*, 4370–4374.
(23) Ruokolainen, J.; Saariaho, M.; Ikkala, O.; ten Brinke, G.; Thomas, E. L.; Torkkeli, M.; Serimaa, R. *Macromolecules* **1999**, *32*, 1152–1158.
(24) Tirumala, V. R.; Daga, V.; Bosse, A. W.; Romang, A.; Ilavsky, J.; Lin, E. K.; Watkins, J. J. *Macromolecules* **2008**, *41*, 7978–7985.
(25) Tirumala, V. R.; Romang, A.; Agarwal, S.; Lin, E. K.; Watkins, J. J. *Adv. Mater.* **2008**, *20*, 1603–1608.
(26) Zhao, Y.; Thorkelsson, K.; Mastroianni, A. J.; Schilling, T.; Luther, J. M.; Rancatore, B. J.; Matsunaga, K.; Jinnai, H.; Wu, Y.; Poulsen, D.; Frechet, J. M. J.; Alivisatos, A. P.; Xu, T. *Nature Mater.* **2009**, *8*, 979–985.
(27) Chen, S. C.; Kuo, S. W.; Jeng, U. S.; Su, C. J.; Chang, F. C. *Macromolecules* **2010**, *43*, 1083–1092.
(28) Sidorenko, A.; Tokarev, I.; Minko, S.; Stamm, M. *J. Am. Chem. Soc.* **2003**, *125*, 12211–12216.
(29) Wang, J.-Y.; Chen, W.; Roy, C.; Sievert, J. D.; Russell, T. P. *Macromolecules* **2008**, *41*, 963–969.
(30) Wang, J.-Y.; Chen, W.; Russell, T. P. *Macromolecules* **2008**, *41*, 4904–4907.
(31) Park, S.; Lee, D. H.; Xu, J.; Kim, B.; Hong, S. W.; Jeong, U.; Xu, T.; Russell, T. P. *Science* **2009**, *323*, 1030–1033.
(32) Wei, X.; Chen, W.; Chen, X.; Russell, T. P. *Macromolecules* **2010**, *43*, 6234–6236.
(33) Kolb, H. C.; Finn, M. G.; Sharpless, K. B. *Angew. Chem., Int. Ed.* **2001**, *40*, 2004–2021.
(34) Rostovtsev, V. V.; Green, L. G.; Fokin, V. V.; Sharpless, K. B. *Angew. Chem., Int. Ed.* **2002**, *41*, 2596–2599.
(35) Tornoe, C. W.; Christensen, C.; Meldal, M. *J. Org. Chem.* **2002**, *67*, 3057–3064.
(36) After the ATRP step, we carefully purified the block copolymer by passing the mixture through a neutral aluminum column to remove the Cu(I) salt. Therefore, click reaction catalyzed by the Cu(I) salt is negligible.
(37) Zhu, L.; Cheng, S. Z. D.; Calhoun, B. H.; Ge, Q.; Quirk, R. P.; Thomas, E. L.; Hsiao, B. S.; Yeh, F. J.; Lotz, B. *J. Am. Chem. Soc.* **2000**, *122*, 5957–5967.
(38) Silvestre, C.; Cimmino, S.; Martuscelli, E.; Karasz, F. E.; Macknight, W. J. *Polymer* **1987**, *28*, 1190–1199.
(39) Russell, T. P.; Ito, H.; Wignall, G. D. *Macromolecules* **1988**, *21*, 1703–1709.
(40) Quiram, D. J.; Register, R. A.; Marchand, G. R.; Adamson, D. H. *Macromolecules* **1998**, *31*, 4891–4898.
(41) Binauld, S.; Boisson, F.; Hamaide, T.; Pascault, J. P.; Drockenmuller, E.; Fleury, E. *J. Polym. Sci., Polym. Chem.* **2008**, *46*, 5506–5517.
(42) Sheng, X.; Mauldin, T. C.; Kessler, M. R. *J. Polym. Sci., Polym. Chem.* **2010**, *48*, 4093–4102.
(43) Sun, S.; Wu, P. *J. Phys. Chem. A* **2010**, *114*, 8331–8336.
(44) Besset, C.; Binauld, S.; Ibert, M.; Fuertes, P.; Pescault, J. P.; Fleury, E.; Bernard, J.; Drockenmuller, E. *Macromolecules* **2010**, *43*, 17–19.
(45) Katritzky, A. R.; Meher, N. K.; Hanci, S.; Gyanda, R.; Tala, S. R.; Mathai, S.; Duran, R. S.; Bernard, S.; Sabri, F.; Singh, S. K.; Doskocz, J.; Ciaramitaro, D. A. *J. Polym. Sci., Polym. Chem.* **2008**, *46*, 238–256.
(46) Hong, S.; MacKnight, W. J.; Russell, T. P.; Gido, S. P. *Macromolecules* **2001**, *34*, 2876–2883.
(47) Loo, Y. L.; Register, R. A.; Adamson, D. H. *Macromolecules* **2000**, *33*, 8361–8366.